AIAA JOURNAL
Vol. 46, No. 6, June 2008

Condition Assessment of Structures Under Ambient White Noise Excitation

X. Y. Li* and S. S. Law†
Hong Kong Polytechnic University,
Hunghom, Kowloon, Hong Kong, People's Republic of China

DOI: 10.2514/1.30426

This paper proposes a damage detection method based on the wavelet packet energy of covariance of measured acceleration responses of structures under ambient excitation. It is a model-based method comparing the measured acceleration responses before and after damage occurrence. The ambient excitation is assumed to be white noise. A damage index based on the change of modal strain energy is used for damage localization. The damage quantification is performed using the sensitivity of the wavelet packet energy of the covariance function. A cantilever five-bay truss structure is used to demonstrate the efficiency of the method with three damage scenarios. The combined two-stage approach is shown capable of locating and accurately quantifying local damages in the presence of measurement noise. A nine-bay three-dimensional truss structure is also assessed in the laboratory with the proposed method, and the whole process of damage detection with incomplete and noisy measurement, initial model error, etc., is demonstrated to be successful for identifying, with good accuracy, local damages in members.

Nomenclature

C	=	damping matrix
$c^i_{j,k}$	=	wavelet packet coefficients at jth level, ith packet, kth time instant
$E(\cdot)$	=	expectation of $(\cdot)$
En^i_j	=	ith wavelet packet transform component energy of the covariance at the jth level
Ep	=	noise level
F_{1i}	=	fractional contribution to the modal strain energy from the ith member
$h(t)$	=	unit impulse displacement
$\dot{h}(t)$	=	unit impulse velocity
$\ddot{h}(t)$	=	unit impulse acceleration
$h_p(t)$	=	vector of impulse response of the system at the pth DOF
K	=	global stiffness matrix
K_i	=	ith elemental stiffness matrix
L	=	mapping vector
M	=	mass matrix
N_{oise}	=	a standard normal distribution vector
ne	=	number of elements in the structure
$R_{pq}(\tau)$	=	cross covariance of accelerations from pth and qth DOF of the system
S	=	magnitude of excitation of $\ddot{x}_s$
S_p	=	energy sensitivity matrix
s_1	=	total modal strain energy of the structure corresponding to the first mode
s_{1i}	=	ith elemental modal strain energy corresponding to the first mode shape
$\text{var}(\cdot)$	=	variance of $(\cdot)$
$\ddot{x}s$	=	ground acceleration.
$x(t)$	=	displacement vector
$\dot{x}(t)$	=	velocity vector
$\ddot{x}(t)$	=	acceleration vector
α_i	=	fractional stiffness of the ith element
$\Delta\alpha_j$	=	jth elemental damage index
$\delta(t)$	=	Dirac delta function
$\frac{\partial(\cdot)}{\partial\alpha_i}$	=	derivative of $(\cdot)$ with respect to α_i
ξ_1, ξ_2	=	Rayleigh damping coefficients
Φ_1	=	first mode shape
$\psi^i_{j,k}$	=	wavelet packet function at jth level, ith packet, kth time instant
$(\cdot)^d$	=	superscript denotes the parameter from the damaged state

Received 14 February 2007; accepted for publication 12 March 2008.

*Ph.D. Student, Civil and Structural Engineering Department.
†Associate Professor, Civil and Structural Engineering Department.

Introduction

EARLY detection of damage in engineering systems during their service life has been receiving increasing attention from researchers in the last few decades. Information on the location and extent of damage could assist in the diagnosis of the structural health conditions and in the recommendation on associated maintenance work. The occurrence of damage in a structure produces changes in its global dynamic characteristics, such as its natural frequencies, mode shapes, modal damping, modal participation factors, impulsive response, and frequency response functions. An understanding of these changes leads to the detection, localization, and characterization of the extent of the damage.

Natural frequencies and mode shapes are usually taken as measured information to identify local damages in frequency domain. However, Farrar et al. [1] showed that the shift of natural frequencies was not sufficiently sensitive to detect local damage in a highway bridge. Mode shapes can also be used to identify and localize damage. However, there are still factors that prevent the general application of the mode shape-based damage detection methods [2].

There is also literature on damage detection directly using structural dynamic response without the need of a modal extraction procedure. Cattarius and Inman [3] used the phase shift in the time history of structural vibration response to identify the presence of damage in smart structures. Majumder and Manohar [4] proposed a time domain approach for damage detection in beam structures using vibration data with a moving oscillator as an excitation source. Choi and Stubbs [5] formed the damage index directly from the time response to locate and quantify damage in a structure. Lu and Gao [6] proposed a new method for damage diagnosis using a time-series analysis of vibration signals, which is formulated in a novel form of the autoregressive exogenous (ARX) model with acceleration response signals. Kang et al. [7] presented a system identification scheme in the time domain to estimate stiffness and damping

parameters of a structure using measured accelerations, and the method is demonstrated with numerical simulation study on a two-span truss bridge and an experimental laboratory study on a three-story shear building model. Later, Law et al. [8] developed the sensitivity-based damage detection method based on the wavelet packet energy of the measured accelerations, and the method can identify damage of a structure from a few measurement locations. More recently, the sensitivity matrix of response with respect to a system parameter is derived analytically [9], but the damage detection results are subject to the effect of measurement noise and model error. These effects on damage identification are further studied with the sensitivity of the wavelet coefficient from structural response [10], with much better results.

However, all of these methods rely on the need for an externally applied excitation. This requirement is not possible in the case of a large civil engineering structure in which a large amount of energy input is required. For large engineering structures, such as bridges, offshore platforms, and high-rise buildings, structural health monitoring based on ambient excitation (environmental excitation or traffic vibration) seems to be the most desirable approach with the advantages of low cost and easy operation. For practical monitoring of operating structures, the ideal system should include noncontact and embedded measurements taken from a structure from excitation under the operation environment, together with automated or semi-automated signal processing [11]. It is noted that most of the existing health monitoring of civil structures is operating continuously, and only ambient excitation can be used for the damage detection of these structures [12].

This paper proposes a damage detection approach based on ambient white noise excitation. The damage severity quantification relies on the measured acceleration responses of the structure before and after damage occurrence. The covariance of "measured" acceleration responses is simulated from finite element analysis. Wavelet packet transform (WPT) is applied to the covariance functions to find the wavelet packet energy. The sensitivity of this packet energy with respect to local damages is used in a linear identification equation for solving the unknowns. A damage index is also proposed for the localization of potential candidates of damage elements before the next state of damage detection. A five-bay cantilever truss structure is used to demonstrate the efficiency of the method with three damage scenarios. The identified results indicate that the two-stage approach can locate and quantify local damages accurately and effectively with no false alarm. A nine-bay experimental structure is also tested with the proposed method and satisfactory results are obtained from using incomplete and noisy measurement and with initial model error.

Theoretical Formulation

Unit Impulse Response Function and Its Sensitivity

The equation of motion of an N degrees-of-freedom (DOF) damped structural system under a unit impulse excitation is

$$M\ddot{x}(t) + C\dot{x}(t) + Kx(t) = -ML\delta(t) \tag{1}$$

where M, C, and K are the $N \times N$ mass, damping, and stiffness matrices, respectively. L is the mapping vector relating the force excitation to the corresponding DOF of the system. The variables $x(t)$, $\dot{x}(t)$, and $\ddot{x}(t)$, are the $N \times 1$ displacement, velocity, and acceleration vectors, respectively. The term $\delta(t)$ is the Dirac delta function. Assuming the system is in static equilibrium before the unit impulse excitation, the system under forced vibration can be converted to a system in free vibration with the following initial conditions:

$$x(0) = 0, \qquad \dot{x}(0) = -ML \tag{2}$$

Rewriting Eqs. (1) and (2), the unit impulse response function can be computed using a time-stepping integral method such as the Newmark method from the following free vibration system:

$$\begin{cases} M\ddot{h}(t) + C\dot{h}(t) + Kh(t) = 0 \\ h(0) = 0, \dot{h}(0) = -ML \end{cases} \tag{3}$$

where $h(t)$, $\dot{h}(t)$, and $\ddot{h}(t)$ are the unit impulse displacement, velocity, and acceleration vectors, respectively.

Because this work is focused on the presentation of a damage detection technique, an approximate model on the local damage is adopted in which the stiffness matrix of the damaged structural system is expressed as

$$K^d = \sum_{i=1}^{\text{ne}} K_i^d = \sum_{i=1}^{\text{ne}} \alpha_i K_i$$

where α_i is the fractional stiffness of an element with $0.0 \le \alpha_i \le 1.0$, and "ne" is the number of elements in the structure. K_i^d represents the ith damaged element stiffness matrix. It is assumed that the local damages would produce a stationary linear effect, which is time invariant. Differentiating Eq. (3) with respect to α_i, we get

$$\begin{cases} M\frac{\partial \ddot{h}}{\partial \alpha_i} + C\frac{\partial \dot{h}}{\partial \alpha_i} + K\frac{\partial h}{\partial \alpha_i} = -\frac{\partial K}{\partial \alpha_i}h - \frac{\partial C}{\partial \alpha_i}\dot{h} \\ \frac{\partial h(0)}{\partial \alpha_i} = 0, \qquad \frac{\partial \dot{h}(0)}{\partial \alpha_i} = -\frac{\partial ML}{\partial \alpha_i} \end{cases} \tag{4}$$

The sensitivities $\frac{\partial h}{\partial \alpha_i}$, $\frac{\partial \dot{h}}{\partial \alpha_i}$, and $\frac{\partial \ddot{h}}{\partial \alpha_i}$ can then be obtained from Eq. (4) with the Newmark method.

Covariance of Acceleration Responses from Structures Under Ambient Vibration

Equation (1) can be rewritten for an N DOF damped structural system under ground ambient excitation as

$$M\ddot{x} + C\dot{x} + Kx = -ML\ddot{x}_s \tag{5}$$

where $\ddot{x}_s$ is the ground acceleration. If the system has zero initial conditions, the solution of Eq. (5) can be expressed as

$$\ddot{x}_p(t) = \int_{-\infty}^{t} \ddot{h}_p(t-\tau)\ddot{x}_s(\tau)\,\mathrm{d}\tau \tag{6}$$

where $\ddot{h}_p(\tau)$ is the impulse response of the pth DOF of the system under the unit impulse excitation. The term $\ddot{x}_p(t)$ represents the acceleration responses from the pth DOF at time t.

If $R_{pq}(\tau)$ denotes the cross covariance of the accelerations from the pth and qth DOF of the system, it can be formulated as follows [13]:

$$R_{pq}(\tau) = E\left\{\int_{-\infty}^{t} \ddot{h}_p(t-\sigma_1) \cdot \ddot{x}_s(\sigma_1)\mathrm{d}\sigma_1 \int_{-\infty}^{t+\tau} \ddot{h}_q(t+\tau-\sigma_2) \cdot \ddot{x}_s(\sigma_2)\,\mathrm{d}\sigma_2\right\} \tag{7}$$

Assuming the deterministic system is subject to random excitation, $\ddot{x}_s(\cdot)$ is random in Eq. (7), and the equation can be rewritten as

$$R_{pq}(\tau) = \int_{-\infty}^{t}\int_{-\infty}^{t+\tau} \ddot{h}_p(t-\sigma_1)\ddot{h}_q(t+\tau-\sigma_2) \cdot E[\ddot{x}_s(\sigma_1)\ddot{x}_s(\sigma_2)]\,\mathrm{d}\sigma_1\,\mathrm{d}\sigma_2 \tag{8}$$

The term $\ddot{x}_s$ is assumed to be of ideal white noise distribution, and the autocorrelation function of $\ddot{x}_s$ is [13]

$$E[\ddot{x}_s(\sigma_1)\ddot{x}_s(\sigma_2)] = S\delta(\sigma_1 - \sigma_2) \tag{9}$$

where S is a constant defining the magnitude of excitation of $\ddot{x}_s$ when $\sigma_1 = \sigma_2$, and $\delta(t)$ is the Dirac delta function. Substituting Eq. (9) into (8) with

$$\int_{-\infty}^{+\infty} f(t)\delta(t)\,\mathrm{d}t = f(0)$$

we have

$$R_{pq}(\tau) = S\int_0^{+\infty} \ddot{h}_s(t)\ddot{h}_q(t+\tau)\,\mathrm{d}t \tag{10}$$

It should be noted that $\ddot{h}_p(t)$ is an intrinsic function of the structure and is dependent only on the excitation location. Equation (10) also shows that $R_{pq}(\tau)$ has the same property as $\ddot{h}_p(\tau)$ or $\ddot{h}_q(\tau)$. The autocorrelation function can be derived in the same way by putting $q = p$ in Eq. (10). Equation (10) can then be computed directly by integration. This formulation relates the cross-correlation function with the physical structural system via the impulse response function.

The sensitivity of the cross-correlation function $R_{pq}(\tau)$ can be obtained from Eq. (10) as

$$\frac{\partial R_{pq}(\tau)}{\partial \alpha_i} = S\left(\int_0^{+\infty} \frac{\partial \ddot{h}_p(t)}{\partial \alpha_i}\ddot{h}_q(t+\tau)\,\mathrm{d}t + \int_0^{+\infty} \ddot{h}_p(t)\frac{\partial \ddot{h}_q(t+\tau)}{\partial \alpha_i}\,\mathrm{d}t\right) \tag{11}$$

where $\frac{\partial \ddot{h}_p(t)}{\partial \alpha_i}$ and $\frac{\partial \ddot{h}_q(t+\tau)}{\partial \alpha_i}$ are obtained numerically from Eq. (4).

Wavelet Packet Energy of Cross Covariance of Acceleration Responses

The covariance of acceleration response obtained here can be represented by Daubechies (db4) wavelet basis function through the dyadic wavelet transformation. The bandwidths of each level of the dyadic wavelet transform are octaves. The wavelet packet transform component function of the covariance $R_{pq}(t)$ can be reconstructed from the wavelet packet coefficients [8] as

$$R^i_{pq,j}(t) = \sum_{k=-\infty}^{+\infty} c^i_{j,k}\psi^i_{j,k}(t) = Q^i_j c^i_j = Q^i_j D^i_j R_{pq}(t) \tag{12}$$

where

$$Q^i_j = \begin{bmatrix} \psi^i_{j,0} & \psi^i_{j,2} & \dots & \psi^i_{j,l} \end{bmatrix}, \qquad (l = 0, 1, \dots, N/2^j - 1)$$

and

$$D^{2i}_{j+1} = H^{j+1}D^i_j$$

$$D^{2i+1}_{j+1} = G^{j+1}D^i_j$$

$D^0_1 = H^1$, $D^1_1 = G^1$, H^{j+1}, and G^{j+1} are matrices formed from the low-pass and high-pass filter functions. The term c^i_j represents the wavelet packet coefficients for the covariance response with $c^i_j = D^i_j R_{pq}(t)$. The ith WPT component energy of the covariance $R_{pq}(t)$ at the jth level of decomposition, En^i_j, is defined as

$$En^i_j = \left(R^i_{pq,j}\right)^T\left(R^i_{pq,j}\right) = R^T_{pq}\left(Q^i_j D^i_j\right)^T\left(Q^i_j D^i_j\right)R_{pq} = R^T_{pq}T^i_j R_{pq} \tag{13}$$

where

$$T^i_j = \left(Q^i_j D^i_j\right)^T\left(Q^i_j D^i_j\right)$$

is not a function of the signal and is determined only by the wavelet type.

The sensitivity of En^i_j with respect to the structural parameters α_k is computed as

$$\frac{\partial En^i_j}{\partial \alpha_k} = \frac{\partial R^T_{pq}}{\partial \alpha_k}T^i_j R_{pq} + R^T_{pq}T^i_j\frac{\partial R_{pq}}{\partial \alpha_k} = 2\frac{\partial R^T_{pq}}{\partial \alpha_k}T^i_j R_{pq} \tag{14}$$

where R^T_{pq} and $\partial R^T_{pq}/\partial \alpha_k$ can be obtained from Eqs. (4), (10), and (11). The sensitivity matrix S_p can then be obtained as

$$S_p = \begin{bmatrix} \frac{\partial En^0_j}{\partial \alpha_k} & \frac{\partial En^1_j}{\partial \alpha_k} & \dots & \frac{\partial En^{2^j-1}_j}{\partial \alpha_k} \end{bmatrix}, \qquad k = 1, 2, \dots, ne \tag{15}$$

and the damage detection can then be performed as follows.

Damage Identification

Damage Localization Based on Mode Shape

The structural modal parameters (mode shape and natural frequencies) can be identified from the ambient vibration responses using the Natural Excitation Technique (NEXT) [14] in conjunction with the Eigensystem Realization Algorithm (ERA) [15], or using the conventional peak-picking technique. The obtained mode shapes Φ are then used for the damage localization as shown next. Because mode shapes of higher order are usually obtained with difficulties in real measurement, only the first mode shape is employed for the damage localization.

The modal strain energy of the ith element corresponding to the first mode shape from the healthy structure is defined as

$$s_{1i} = \Phi^T_1 K_i \Phi_1 \tag{16}$$

where K_i is the ith elemental stiffness matrix written in all structural DOF, and Φ_1 is the first mode shape of the system. Then the total modal strain energy of the structure corresponding to the first mode is obtained as

$$s_1 = \Phi^T_1 K \Phi_1 \tag{17}$$

The fractional contribution to the modal strain energy from the ith member is denoted as

$$F_{1i} = \frac{s_{1i}}{s_1} \tag{18}$$

Similarly, for a damaged structure, the corresponding F^d_{1i} is defined as

$$F^d_{1i} = \frac{s^d_{1i}}{s^d_1} \tag{19}$$

where

$$s^d_{1i} = \left(\Phi^d_1\right)^T K^d_i \Phi^d_1 \tag{20}$$

and

$$s^d_1 = \left(\Phi^d_1\right)^T K^d \Phi^d_1 \tag{21}$$

where K^d_i and K^d are the ith elemental stiffness matrix and the global stiffness matrix of the damaged structure, respectively. The variable Φ^d_1 is the first mode shape of the damaged structure.

Equation (20) can be expressed as

$$s^d_{1i} = \alpha_i\left(\Phi^d_1\right)^T K_i \Phi^d_1 \tag{22}$$

For the case with relatively small damage in the structure, it can be assumed that

$$F_{1i} \approx F^d_{1i} \tag{23}$$

Based on the assumption of small damage in the structure, $K^d \approx K$, and we have

$$s^d_1 = \left(\Phi^d_1\right)^T K^d \Phi^d_1 \approx \left(\Phi^d_1\right)^T K \Phi^d_1 \tag{24}$$

Substituting Eqs. (16–21) into Eq. (23) yields a damage index as

$$\Delta\alpha_i = 1 - \frac{\left(\Phi^T_1 K_i \Phi_1\right)\left[\left(\Phi^d_1\right)^T K \Phi^d_1\right]}{\left[\left(\Phi^d_1\right)^T K_i \Phi^d_1\right]\left(\Phi^T_1 K \Phi_1\right)} \tag{25}$$

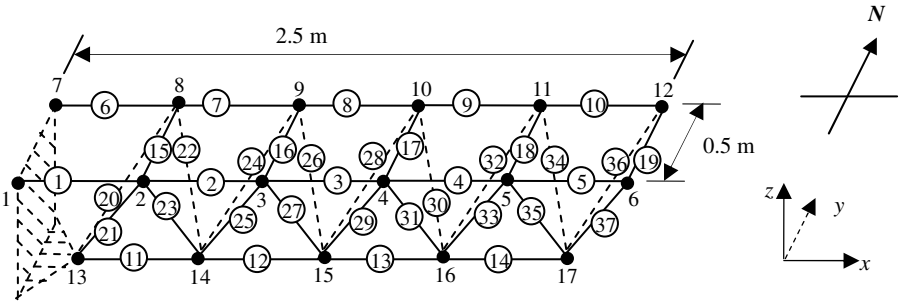

Fig. 1 A five-bay, three-dimensional frame structure.

It is noted that this formulation on the damage index needs full measurement to obtain the mode shape. In the case of incomplete measurement, the measured information can be expanded to the full mode shape, or only the measured information is taken into account in Eq. (25). Both of these practices would lead to errors of different extent, which is a feature with a mode shape-based approach. It should be stated here that the localization stage serves to reduce the candidate set of possible damage elements for the next stage of damage quantification. Other frequency-based or time-based methods can also be used for this purpose.

Damage Severity Identification Based on Sensitivity of the Covariance

Because two assumptions have been made in Eqs. (23) and (24), the damage severity obtained from Eq. (25) is not accurate. A refined damage severity quantification method based on the sensitivity of the covariance with the reduced set of possible damaged elements is pursued here. We consider a general structure that behaves linearly before and after the occurrence of damage for the illustration of the proposed approach. The study of a nonlinear system with time-varying damage model is not included in this study, as it involves a different treatment of the identification problem.

The damage quantification method includes two separate phases of updating the analytical model and identifying local damages. Each phase consists of the two stages of damage localization and quantification. Both $(En_j)_0$ and $(En_j)_d$ are vectors of the WPT component energy of the covariance of the acceleration responses at the pth and qth DOF of the intact and damaged structures, respectively. S_p is the sensitivity matrix of the WPT component energy calculated from the intact state of the system using Eq. (15), and $\Delta\alpha$ is the vector of fractional change of the parameters of the system. We have the identification equation as

$$S_p \cdot \Delta\alpha = (En_j)_d - (En_j)_0 \tag{26}$$

Because the solution of Eq. (26) is ill conditioned, regularization is used with the L-curve method for determining the optimal regularization parameter [8].

The initial analytical model is adopted for model updating in the first stage of the study. Vector $(En_j)_0$ and matrix S_p are obtained from this initial model. Acceleration measurement from the intact state of the structure is obtained, and the covariance, as well as its WPT component energy vector $(En_j)_d$, is computed. The initial model is then updated in Eq. (26), and the corresponding $(En_j)_0$ and its sensitivity S_p are again computed from the updated model for the next iteration. The final updated analytical model is obtained when both of the following two criteria are met:

$$\frac{\|\{En_j\}_{m+1} - \{En_j\}_m\|}{\|\{En_j\}_{m+1}\|} \le \text{toler 1}$$

$$\frac{\|\{\Delta\alpha_{m+1}\} - \{\Delta\alpha_m\}\|}{\|\{\Delta\alpha_{m+1}\}\|} \le \text{toler 2}$$

where m refers to the mth iteration, and toler 1 and toler 2 are the two specified criteria of convergence.

Then the updated analytical model is used to represent the first (intact) state of the structure, and the damaged state of the real structure is regarded as the second state in the identification. Measurement from the damaged state is obtained, and the same iteration computations as in the first stage are carried out. The final set of identified parameter increments correspond to the changes occurred in between the intact and damaged states of the structure.

Numerical Study

A five-bay, three-dimensional frame structure as shown in Fig. 1 serves for the numerical study. The finite element model consists of 37 three-dimensional Euler beam elements and 17 nodes. The length of all the horizontal, vertical, and diagonal tube members between the centers of two adjacent nodes is exactly 0.5 m. The structure orientates horizontally and is fixed into a rigid support at three nodes at one end. The mass of every joint includes the total weight of the ball and half of the weight of the bolt connecting the ball with the frame element. The Meroform ball joints are treated as rigid joints initially, and no additional rigidity is added. Table 1 gives a summary of the main material and geometrical properties of the members of the frame structure. Each node has six DOF, and all together, there are 102 DOF for the whole structure.

The translational and rotational restraints at the supports are represented by large stiffnesses of 1.5×10^{11} kN/m and 1.5×10^{10} kN · m/rad, respectively, in six directions. Rayleigh damping is adopted for the system with $\xi_1 = 0.01$ and $\xi_2 = 0.005$. The first 12 natural frequencies of the intact structure are 9.21, 28.26, 33.71, 49.01, 49.72, 71.02, 89.80, 153.93, 194.33, 209.80, 256.51, and 274.82 Hz from the eigenvalue analysis of the structure. The sampling frequency is 500 Hz.

The finite element model of the structure is used directly for the identification without updating. The structure is subject to the ideal white noise support motion in the y direction with zero mean and a magnitude of 0.01 m^2/s^4. The first mode shape is obtained before and after damage occurrence for localizing the damages. The acceleration responses from nodes 5 and 6 in the y direction are calculated for a duration of 300 seconds from the healthy and the damaged structure for the calculation of the cross covariance to simulate the measured acceleration responses. Three damage cases shown in Table 2 are studied to illustrate the proposed approach.

The flexural stiffness (modulus of elasticity) of element 2 is reduced by 10% in damage scenario 1. To analyze the error introduced by the assumption in Eq. (23), the fractional contributions of the modal strain energy F_{1i} and F_{1i}^d for the intact state and the

Table 1 Material and geometrical properties for one frame member

Properties	Member
Young modulus, N/m^2	2.10E11
Area, m^2	6.597E − 5
Density, kg/m^3	1.2126E4
Mass, kg	0.32
Poisson ratio	0.30
Moment of area I_y, m^4	3.645E − 9
Moment of area I_z, m^4	3.645E − 9
Torsional rigidity J, m^4	7.290E − 9

Table 2 Damage scenarios

Scenario	Damaged member	Damage severity	Noise in acceleration responses
1	2nd element	10%	No
2	12th, 16th, 25th, and 27th elements	5, 5, 5, and 10%	No
3	12th, 16th, 25th, and 27th elements	5, 5, 5, and 10%	10%

damage state, respectively, are computed and compared with $\|(F_{1i}^d - F_{1i})/F_{1i}\|$, and the result is shown in Fig. 2a. It shows that the error caused by the assumption is less than 4% in this case. The damage localization vector is obtained by using all the translational and rotational DOF of the first mode shape. The vector shown in Fig. 2b is not accurate, although it still can identify the range of the damage location. However, there exist false alarms in elements 7, 22, 23, 24, and 25. These elements are noted to be adjacent to and in the same bay as the damaged element. The cross covariance is calculated from the measured acceleration responses and is decomposed by Daubechies (db4) wavelet in four levels with 16 wavelet packets. All the 16 WPT component energies constitute the measurement vector, and 16 equations are used in the identification. Elements 2, 7, 22, 23, 24, and 25 are chosen to be the possible candidates for the next stage of quantification. The identified results from using the covariance sensitivity approach in Eq. (26) are shown in Fig. 2c, indicating that the damage severity of element 2 can be obtained accurately without false alarming in other elements.

To study the case of multiple damages in different types of elements, damage scenario 2 is studied, in which the flexural stiffness of elements 12, 16, and 25 are reduced by 5%, and that in element 27 is reduced by 10%. The fractional contribution F_{1i}^d is computed and compared with F_{1i} as for damage scenario 1. The error introduced by the assumption in Eq. (23) has a maximum of 4.96% as shown in Fig. 3a. The damage localization vector is computed similarly and shown in Fig. 3b from which it can be seen that the assumption is valid, but it affects the accuracy of the identified results. The identified damage localization vector contains both the real damage locations and false alarms in adjacent elements. These results are useful for the damage quantification because the group of possible candidate has been reduced. Elements 12, 16, 24, 25, 26, and 27 are chosen as the possible damage elements for the quantification identification. The identified damage magnitudes are shown in Fig. 3c, and they are very accurate.

Despite the capability of the cross-covariance computation in reducing the noise effect, 10% noise is added to the measured acceleration responses whereas the damage elements and severity are the same as in scenario 3. White noise is added to the calculated accelerations to simulate the polluted measurements as follows:

$$\ddot{x}_{\text{measured}} = \ddot{x}_{\text{calculated}} + Ep^* N_{\text{oise}}^* \text{var}(\ddot{x}_{\text{calculated}})$$

where $\ddot{x}_{\text{measured}}$ is the vector of polluted acceleration, Ep is the noise level, N_{oise} is a standard normal distribution vector with zero mean value and unit standard deviation, var$(\cdot)$ is the variance of the time history, and $\ddot{x}_{\text{calculated}}$ is the vector of measured acceleration. This forms scenario 3 in Table 2. The identified damage magnitudes are also shown in Fig. 3c for comparison with those without noise. The identified results are noted to be only slightly affected with noise in the measured acceleration.

It is always noted that the effect of model error would smear the identified damages throughout the structure with many of the existing damage quantification methods giving false alarms in other undamaged elements. This is a matter of accuracy with the

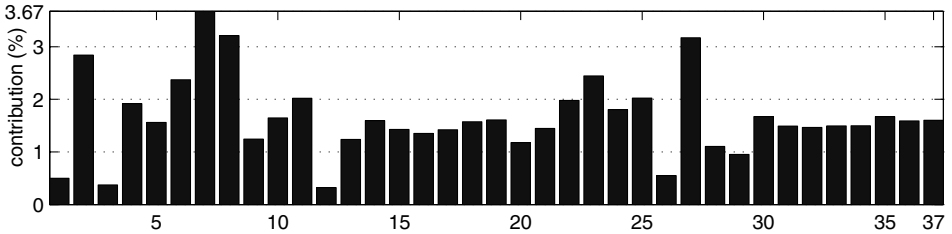

a) Contribution from intact and damaged states

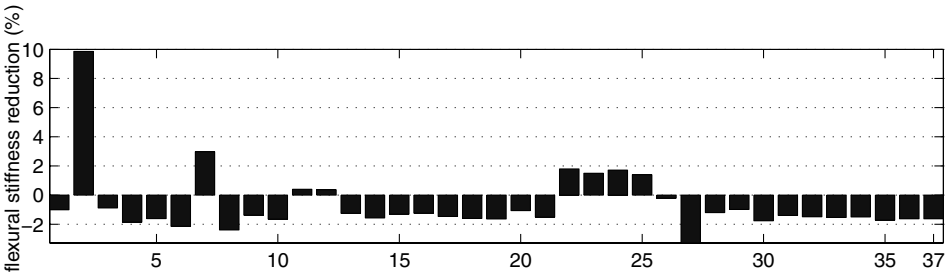

b) Damage localization vector

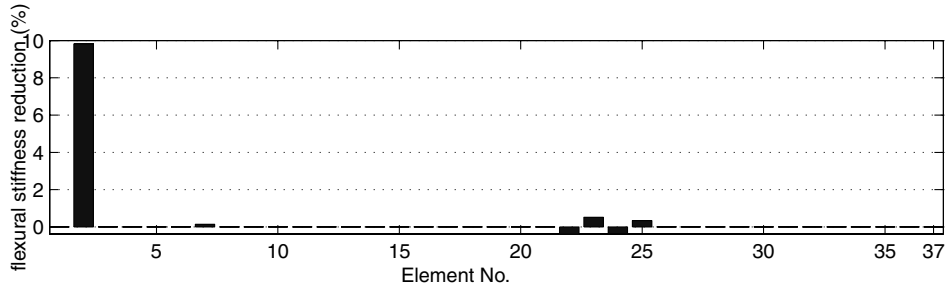

c) Damage extent vector

Fig. 2 Identified results for damage scenario 1.

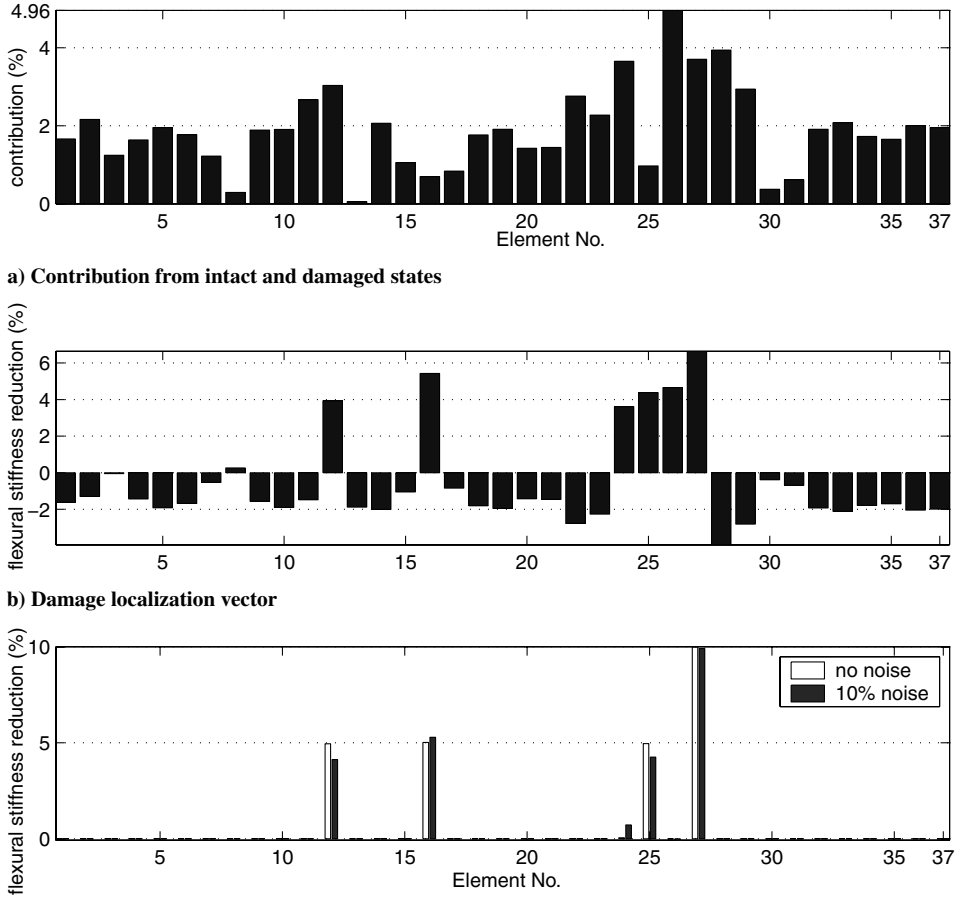

a) Contribution from intact and damaged states

b) Damage localization vector

c) Damage extent vector

Fig. 3 Identified results for damage scenarios 2 and 3.

identification method. Experiences with the authors when using the wavelet approach for the damage identification [10] show that model errors related to the stiffness terms of the structure can also be identified as local damages whereas those related to the mass or damping terms would not show up clearly because of the lack of a clear relationship between the measured responses and these parameters with existing methods.

Discussion

The results shown in Figs. 2 and 3 indicate that the covariance approach can quantify local damage accurately provided that the number of unknowns in the identification is small. This can be improved by using more sets of covariance responses from different pairs of measured acceleration time histories. However, the inclusion of the localization stage could eliminate some intact elements, leaving a smaller candidate set of unknowns for a more accurate damage quantification in the next stage.

In the case of a structure in which a few critical components are needed to be monitored continuously, the proposed covariance approach would be most suitable provided that a satisfactory finite element model of the intact structure has been updated before the implementation of the structural health monitoring.

Experimental Verification

A nine-bay three-dimensional frame structure shown in Fig. 4a serves for the experimental study. It was fabricated in the laboratory using Meroform M12 construction system. It consists of 69 22-mm-diam alloy steel tubes jointed together by 29 standard Meroform ball nodes. Each tube is fitted with a screwed end connector that, when tightened into the node, also clamps the tube by means of an internal compression fitting. All the connection bolts are tightened with the same torsional moment to avoid asymmetry or nonlinear effects caused by man-made assembly errors. The experimental setup is also shown in Fig. 4a, and the support is shown in Fig. 4b. The finite element model of the structure is shown in Fig. 5. The structure has the same material and geometric properties as shown in Table 1.

Modal Test

The modal test on both the intact and damaged structure is performed using the single-input–multiple-output method with a dynamic hammer model B&K 8202 hitting on element 10 along the y direction and close to node 11 of the frame. A total of 52 translation DOF at the unconstrained nodes are measured. An additional mass of 72 g weight is added to each joint to balance the effect of the moving accelerometers. The sampling frequency is 2000 Hz. The responses are low-pass filtered at 1000 Hz, and a commercial data logging system INV303 with the associated data analysis system DASP2003 is used in the data acquisition. The frequency response function (FRF) is calculated for all the measured responses, and the first 12 natural frequencies and modal damping ratios that averaged over 20 FRFs are listed in the fourth and fifth columns of Table 3. The corresponding measured mode shapes are given in Fig. 6. Only a few pure bending modes are identified, whereas most of them have coupled bending and torsional vibrations.

Modeling of Structure

The authors have treated the Meroform ball joints as semirigid joints, and a finite element model of a hybrid beam with semirigid end connections has been proposed [16]. This paper adopts this hybrid beam model for the model improvement of the structure. The initial model assumes a large fixity factor p for the rotational stiffness of the joints, which is taken equal to 0.999 with 1.0 equal to that for a rigid joint.

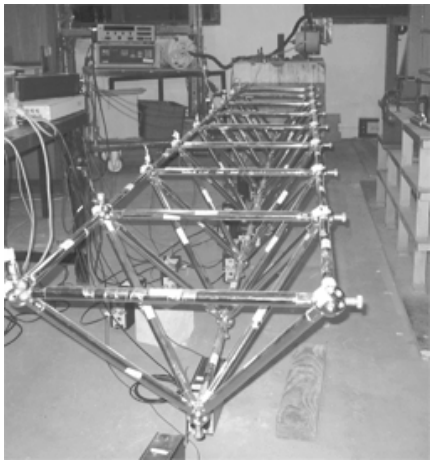

a) The cantilevered 3D steel tube frame structure

b) The rigid concrete support and the actuator

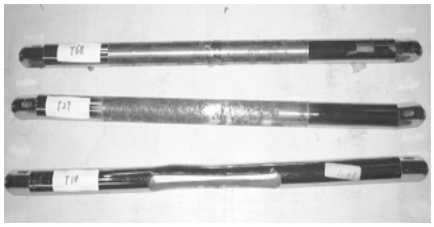

c) The damaged elements

Fig. 4 Experimental setup and the damaged elements of the nine-bay frame structure.

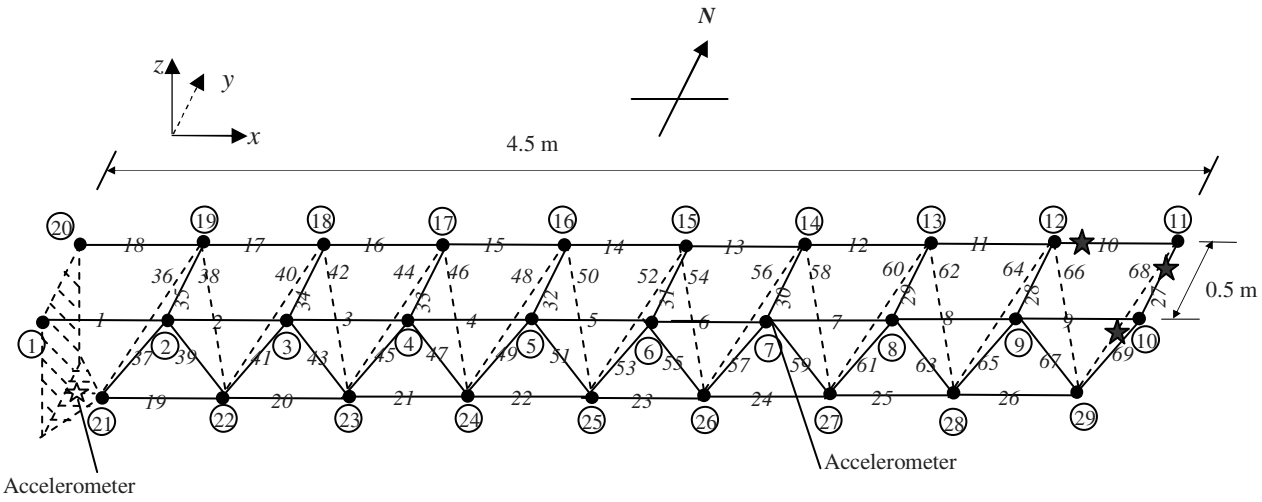

Fig. 5 A nine-bay three-dimensional frame structure (★ is a damaged element).

Table 3 The natural frequencies (Hz) and damping ratio of the frame structure

Mode type	FEM		Measured			
	Frequency, Hz/error, %		Intact		Damaged	
	Intact	Stage 1	Frequency, Hz	Damping ratio	Frequency, Hz	Damping ratio
1H	5.207	5.165/ − 0.58%	5.196	0.443	5.216	0.196
1V	11.076	10.951/0.09%	10.942	0.928	10.794	0.418
2H	15.305	15.063/ − 0.72%	15.172	0.282	15.166	0.251
V + T	19.493	19.276/ − 0.59%	19.390	0.155	19.387	0.155
3H	27.888	27.646/ − 0.20%	27.702	0.307	27.462	0.299
H	40.211	39.445/ − 0.93%	39.815	0.335	39.127	0.346
H	53.234	52.203/0.11%	52.146	0.423	51.018	0.403
2V	61.565	61.517/ − 0.68%	61.938	0.155	61.463	0.432
H + T	66.979	65.655/ − 0.23%	65.806	0.258	64.142	0.253
H + T	80.706	79.088/0.76%	78.491	0.356	76.616	0.333
T	88.239	87.462/0.20%	87.287	0.908	89.277	0.333
H + T	93.269	91.334/0.98%	90.448	0.340	98.125	0.312

2H is second horizontal mode; 1V is first vertical mode; V + T is coupled vertical and torsional mode.

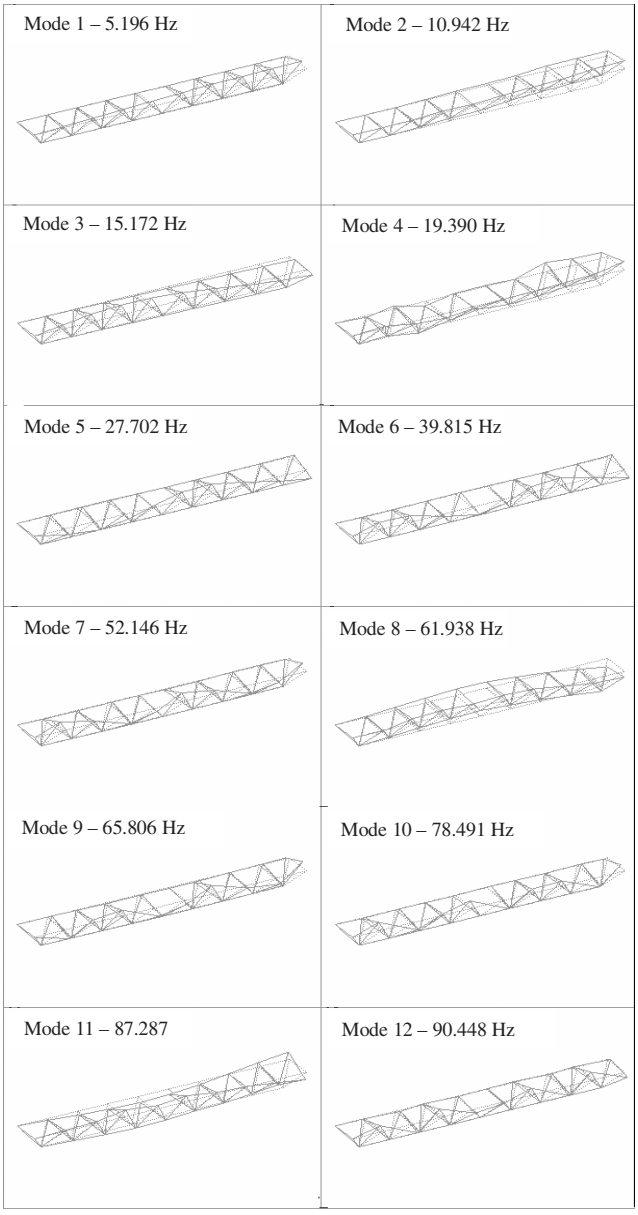

Fig. 6 Measured mode shapes of the intact steel frame structure.

The total weight of the ball and half of the weight of the bolt connecting the ball with the frame element are placed at each node as lump mass. The other half of the weight of the bolt is considered as part of the finite element. In additional, another lump mass of 72 g weight is added to each node to represent the weight of the moving accelerometers. The natural frequencies calculated from the finite element model are shown in column two of Table 3, which are very close to the measured values.

Ambient Vibration Test for Damage Detection

The structure is excited with a random white noise signal through a LING PO 300 exciter approximately at the centroid of the support in the y direction. The support is very rigid and heavy compared with the frame, and it is held down to the strong floor with four steel bolts. The acceleration responses of the support along the three principal directions are measured. Only the response in the y direction is significant, and those in the other two directions are small enough to be neglected. Nine accelerometers are placed at nodes 2 to 10 in the y direction for recording the acceleration response time histories. The sampling frequency is 2000 Hz, and the responses for a duration of 800 s are used to calculate the autocovariance. The autocovariance of acceleration time history at the support in the y direction has a magnitude of 0.0031 m^2/s^4 at $t = 0$ and small values for other time instances as shown in Fig. 7a, indicating a close to white noise excitation at the support [Eq. (9)]. The autocovariance of acceleration time history from node 8 before and after the damage occurrence is shown in Figs. 7b and 7c, respectively. The covariances are noted to be relatively smooth with a low noise level.

Damage Scenarios

After performing the dynamic test on the intact frame structure, local faults are introduced by replacing three intact members with damaged ones. The artificial damage is of two types. Type 1 is a perforated slot cut in the central length of the member. The length of slot is 13.7 cm, and the remaining depth of the tube in the cross-cut section is 14.375 mm. Type 2 is the removal of a layer of material from the surface of the member. The external diameter of the tube is reduced from 22.02 to 21.47 mm, and the length of the weakened section is 202 mm, located in the middle of the beam, leaving 99 and 75 mm length of original tube cross section on both sides. Figure 4c gives a close up view of the damaged frame members. Type 1 damage is located in element 10, and type 2 damage is located in elements 27 and 68. The equivalent damages computed by Guyon method are 5 and 9.5% reduction in the modulus of elasticity of element 10 and elements 27 and 68, respectively. Modal test is again performed on this structure, and the natural frequencies and modal damping ratios obtained are shown in columns six and seven of Table 3.

Model Improvement for Damage Detection

The two-stage approach is adopted for the damage detection. The first stage updates the rotational stiffness at the joints to obtain an improved analytical model for the intact structure. Nine y-direction acceleration responses obtained from nodes 2 to 10 are measured, and the corresponding autocovariance WPT energy components are computed for use in Eq. (26). There are $69 \times 6 = 414$ unknown rotational stiffnesses in the identification. The first 2000 data points of autocovariance of each acceleration response are decomposed into six levels of Daubechies db4 wavelet packets to have 64 covariance WPT energy components, and each packet has the same frequency bandwidth of 15.625 Hz. All the 64 WPT energy components are used in the experimental identification procedure, and there are $9 \times 64 = 576$ equations in Eq. (26). The measured modal damping ratios from the intact structure have been used in Eqs. (1) and (5) for the computation of the analytical autocovariance. The updated rotational stiffness does not differ too much from the original value, with the largest change in member 20 at node 22, with the updated $p = 0.86$ for the x-axis rotational stiffness. The natural frequencies calculated from this updated finite element model are shown in column three of Table 3. Compared with the measured values from the intact state, the errors shown are all smaller than 1%, indicating that this updated model is accurate enough for the next stage of damage assessment.

The second stage updates the local faults in all the members of the structure in terms of their modulus of elasticity. The damage localization is performed first. The measured first mode shape with 52 translational DOF from the intact and the damaged states of the structure are expanded to the full degrees of freedom by the dynamic condensation method with Gauss–Jordan elimination [17], and the obtained damage localization vector is shown in Fig. 8a, indicating that the real damaged members can be identified but with false alarms in other undamaged members because of the error due to measurement noise and the mode shape expansion.

The autocovariance calculated from the y-direction response from nodes 2 and 10 is used in Eq. (26) for the identification. There are 26 unknowns, which are the suspected damaged elements shown in Fig. 8a in the identification. The first 2000 data points of autocovariance of each response are used, and all $64 \times 9 = 576$ WPT energy components are used in Eq. (26). The identified damage extent for all the elements is shown in Fig. 8b. The identified reduction in the modulus of elasticity in the damaged members is 4.76, 7.09, and 6.73% for elements 10, 27, and 68, respectively,

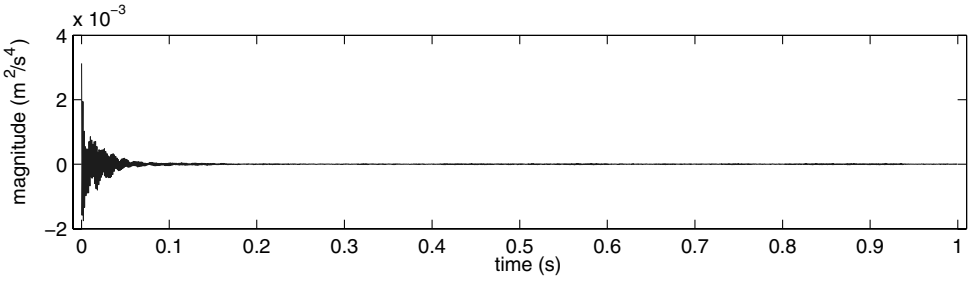

a) Autocovariance of y−direction response from support

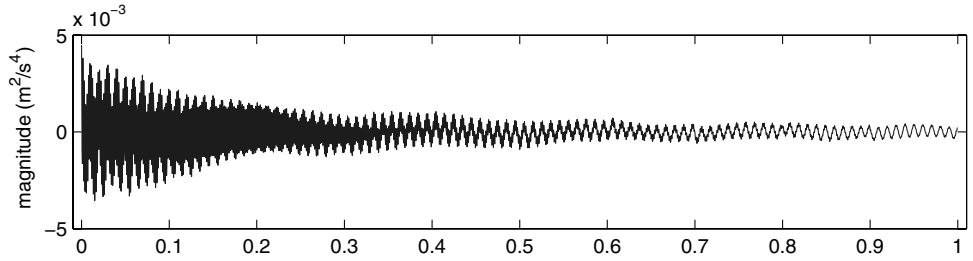

b) Autocovariance of y−direction response from Node 8 in the intact state

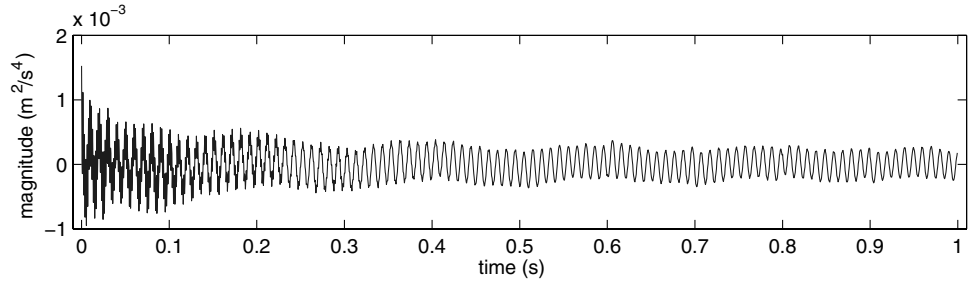

c) Autocovariance of y−direction response from Node 8 in the damaged state

Fig. 7 Autocovariance of accelerations at support and structure.

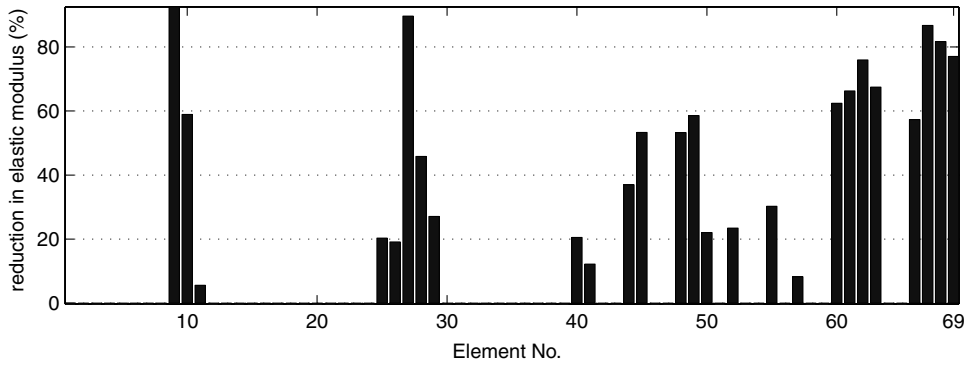

a) Damage localization vector

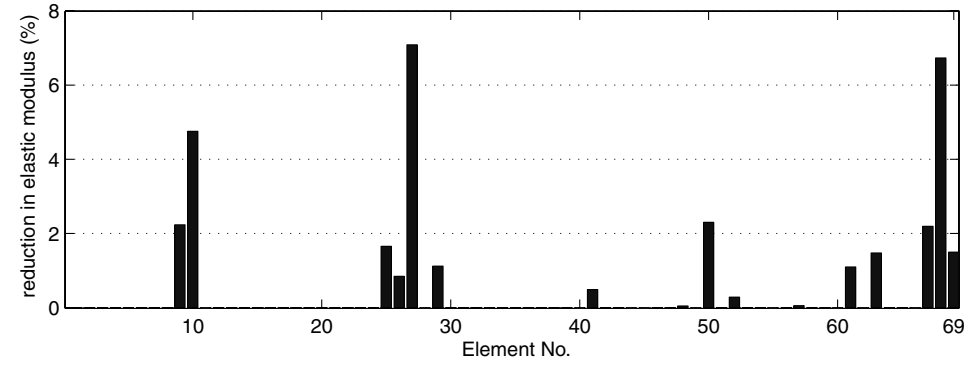

b) Damage extent vector

Fig. 8 Identified results for the experimental structure.

which are fairly close to the values of 5, 9.5, and 9.5%, respectively. There are false alarms in elements 9, 50, and 67, with a reduction of more than 2% even though they are, in fact, undamaged.

Further attempts have been made in using accelerations from three, five, and seven sensors in the same group of sensors in the identification. The accuracy of the identified results is poorer than the previously mentioned one. The combination of accelerations in both the vertical and lateral directions may be a better one, but it has not been studied because of limitations with the test results. It may be concluded from the limited study that the measurement noise and model errors have a significant effect on the identification with the proposed identification method using random input excitation.

It should be noted that the selection of damage elements at the end of the cantilever is due to the consideration of experimental ease and assembly repeatability. It also carries an intention to identify a damage scenario with damage elements experiencing a small change in the stress and strain, which is usually difficult to be identified with existing techniques.

Conclusions

This paper proposed a damage detection method based on the wavelet packet energy of the covariance calculated from the measured acceleration responses of structures under ambient excitation that is assumed to be white noise. Wavelet packet transform is applied to the covariance functions to find the wavelet packet energy. To reduce the number of the unknowns involved in the inverse problem, damage localization is carried out first using the elemental modal strain energy. The much-reduced set of potential damage elements then undergoes the next stage of damage quantification. The proposed damage quantification method based on the sensitivity of the wavelet packet transform energy of covariance has good capability in dealing with model error and measurement noise. A five-bay, three-dimensional cantilever truss structure is used to demonstrate the efficiency of the method with three damage cases. A nine-bay three-dimensional frame structure is also assessed in the laboratory with the proposed method, and the identified results show that the method is applicable to locate and quantify local damages with incomplete and noisy measurement and with initial model error.

Acknowledgment

The work described in this paper was supported by a research grant from the Hong Kong Polytechnic University.

References

[1] Farrar, C. R., Baker, W. E., Bell, T. M., Cone, K. M., Darling, T. W., Duffey, T. A., Eklund, A., and Migliori, A., "Dynamic Characterization and Damage Detection in the I-40 Bridge over the Rio Grande," Los Alamos National Laboratory Report LA-12767-MS, 1994.

[2] Chance, J., Tomlinson, G. R., and Worden, K., "A Simplified Approach to the Numerical and Experimental Modeling of the Dynamics of a Cracked Beam," *Proceeding of the 12th International Modal Analysis Conference*, Society for Experimental Mechanics, Bethel, CT, 1994, pp. 778–785.

[3] Cattarius, J., and Inman, D. J., "Time domain analysis for damage detection in smart structures," *Mechanical Systems and Signal Processing*, Vol. 11, No. 3, 1997, pp. 409–423. doi:10.1006/mssp.1996.0086

[4] Majumder, L., and Manohar, C. S., "A Time Domain Approach for Damage Detection in Beam Structures Using Vibration Data with a Moving Oscillator as an Excitation Source," *Journal of Sound and Vibration*, Vol. 268, No. 4, 2003, pp. 699–716. doi:10.1016/S0022-460X(02)01555-9

[5] Choi, S., and Stubbs, N., "Damage Identification in Structures Using the Time-Domain Response," *Journal of Sound and Vibration*, Vol. 275, Nos. 3–5, 2004, pp. 577–590. doi:10.1016/j.jsv.2003.06.010

[6] Lu, Y., and Gao, F., "A Novel Time-Domain Auto-Regressive Model for Structural Damage Diagnosis," *Journal of Sound and Vibration*, Vol. 283, Nos. 3–5, 2005, pp. 1031–1049. doi:10.1016/j.jsv.2004.06.030

[7] Kang, J. S., Park, S. K., Shin, S., and Lee, H. S., "Structural System Identification in Time Measured Acceleration," *Journal of Sound and Vibration*, Vol. 288, Nos. 1–2, 2005, pp. 215–234. doi:10.1016/j.jsv.2005.01.041

[8] Law, S. S., Li, X. Y., Zhu, X. Q., and Chan, S. L., "Structural Damage Detection from Wavelet Packet Sensitivity," *Engineering Structures*, Vol. 27, No. 9, 2005, pp. 1339–1348. doi:10.1016/j.engstruct.2005.03.014

[9] Law, S. S., and Lu, Z. R., "State-Space Approach to Calculate Sensitivity of Dynamic Response," *Symposium on Advances in System Identification Techniques*, Vol. 255, Technical Committee on Vibration and Sound, ASME Design Engineering Division Dynamics and Control of Structures and Systems Committee, American Society of Mechanical Engineers Applied Mechanics Division, Fairfield, NJ, 2004, pp. 109–112.

[10] Law, S. S., and Li, X. Y., "Structural Damage Detection from Wavelet Coefficient Sensitivity with Model Errors," *Journal of Engineering Mechanics*, Vol. 132, No. 10, 2006, pp. 1077–1087. doi:10.1061/(ASCE)0733-9399(2006)132:10(1077)

[11] Farrar, C. R., and Doebling, S. W., "Lessons Learned from Applications of Vibration-Based Damage Identification Methods to Large Bridge Structures," Structural Health Monitoring: Current Status and Perspectives, *Proceedings of the International Workshop on Structural Health Monitoring*, Technomic, Lancaster, PA, 1997, pp. 351–370.

[12] Peters, B., *System Identification and Damage Detection in Civil Engineering*, Ph.D. Thesis, Department of Civil Engineering, Katholieke Universiteit Leuven, Leuven, Belgium, 2000.

[13] Bendat, J. S., and Piersol, A. G., *Engineering Applications of Correlation and Spectral Analysis*, Wiley, New York, 1980.

[14] James, G. H., III., Carne, T. G., and Lauffer, J. P., "The Natural Excitation Technique (Next) for Modal Parameters Extraction from Operating Structures," *Modal Analysis: the International Journal of Analytical and Experimental Modal Analysis*, Vol. 10, No. 4, 1995, pp. 260–277.

[15] Juang, J. N., and Pappa, R. S., "An Eigensystem Realization Algorithm for Modal Parameters Identification and Model Reduction," *Journal of Guidance, Control, and Dynamics*, Vol. 8, No. 5, 1985, pp. 620–627.

[16] Law, S. S., Chan, T. H. T., and Wu, D., "Super-Element with Semi-Rigid Joints in Model Updating," *Journal of Sound and Vibration*, Vol. 239, No. 1, 2001, pp. 19–39. doi:10.1006/jsvi.2000.3110

[17] Mario, P., *Structural Dynamics: Theory and Computation*, Chapman and Hall, New York, 1997.

N. Alexandrov
Associate Editor